JOURNAL OF GUIDANCE, CONTROL, AND DYNAMICS
Vol. 33, No. 2, March–April 2010

Airspace Encounter Models for Estimating Collision Risk

Mykel J. Kochenderfer,* Matthew W. M. Edwards,† Leo P. Espindle,‡ James K. Kuchar,§ and J. Daniel Griffith¶
Massachusetts Institute of Technology, Lexington, Massachusetts 02420

DOI: 10.2514/1.44867

Airspace encounter models, providing a statistical representation of geometries and aircraft behavior during a close encounter, are required to estimate the safety and robustness of collision avoidance systems. Prior encounter models, developed to certify the Traffic Alert and Collision Avoidance System, have been limited in their ability to capture important characteristics of encounters as revealed by recorded surveillance data, do not capture the current mix of aircraft types or noncooperative aircraft, and do not represent more recent airspace procedures. This paper describes a methodology for encounter model construction based on a Bayesian statistical framework connected to an extensive set of national radar data. In addition, this paper provides examples of using several such high-fidelity models to evaluate the safety of collision avoidance systems for manned and unmanned aircraft.

Nomenclature

A	=	airspace class (i.e., B, C, D, or other)
C	=	category of aircraft (i.e., discrete or 1200 code)
D	=	data
G	=	graphical structure of a Bayesian network
$\dot{h}$	=	vertical rate
hmd	=	horizontal miss distance at time of closest approach
L	=	altitude layer
N_{ijk}	=	observed number of times the ith variable was assigned to its kth value when the values of its parents correspond to their jth collective instantiation
$p(\boldsymbol{z})$	=	distribution over encounters
$q(\boldsymbol{z})$	=	sampling distribution over encounters
q_i	=	number of possible instantiations for the parents of the ith variable
r_i	=	number of possible values for the ith variable
t	=	time
v	=	airspeed
$\dot{v}$	=	airspeed acceleration
vmd	=	vertical miss distance at time of closest approach
$\boldsymbol{z}$	=	encounter
$\boldsymbol{z}^{(i)}$	=	ith encounter sample
α_{ijk}	=	kth parameter in the Dirichlet distribution over the ith variable when the values of its parents correspond to their jth collective instantiation
β	=	approach angle at time of closest approach
$\boldsymbol{\pi}_i$	=	parental instantiation of the ith variable
χ	=	bearing of intruder relative to own aircraft at time of closest approach
$\dot{\psi}$	=	turn rate

Received 14 April 2009; revision received 20 November 2009; accepted for publication 20 November 2009.

*Technical Staff, Lincoln Laboratory, Surveillance Systems, 244 Wood Street; mykelk@ll.mit.edu. Member AIAA.

†Associate Staff, Lincoln Laboratory, Surveillance Systems, 244 Wood Street; matthew.edwards@ll.mit.edu. Member AIAA.

‡Assistant Staff, Lincoln Laboratory, Surveillance Systems, 244 Wood Street; espindle@ll.mit.edu. Member AIAA.

§Associate Group Leader, Lincoln Laboratory, Weather Sensing, 244 Wood Street; kuchar@ll.mit.edu. Associate Fellow AIAA.

¶Associate Staff, Lincoln Laboratory, Surveillance Systems, 244 Wood Street; dan.griffith@ll.mit.edu. Member AIAA.

I. Introduction

RIGOROUS analysis of a collision avoidance system is required before deployment in the airspace due to the potentially catastrophic consequences of error in their operation. Civil aviation authorities, such as the Federal Aviation Administration (FAA) and Eurocontrol, require a combination of flight tests and detailed simulation studies to ensure system effectiveness and safety. Although a flight test can evaluate a system in actual operation, only a relatively few situations can be examined because of time, cost, and safety constraints. Simulation studies are required to test the robustness of the system over a significantly wider range of situations. These situations, in turn, need to be generated by a statistical model of encounters that are representative of what actually occurs in the airspace. Sampling a large collection of situations from such an encounter model and running them in simulation both with and without a collision avoidance system provides an estimate of the differential in collision risk.

Estimated risk depends strongly on the distribution of the encounters represented by the model. Hence, it is important that the encounter geometries and aircraft behavior represented by the model be as representative of the actual airspace as possible; otherwise, the risk associated with a collision avoidance system could be significantly over- or underestimated. To ensure a representative model, a large collection of recorded surveillance data is typically used to extract state probabilities over various encounter variables.

Several encounter models have been previously developed by various organizations to support the development of the Traffic Alert and Collision Avoidance System (TCAS) since the mid-1980s [1–8]. These encounter models are based primarily on radar data. To provide sufficient time for TCAS to detect and avoid an intruder, the encounter models represent the motion of two aircraft during the last minute (approximately) before the time of closest approach. The encounter models are designed to be simple enough to permit fast-time Monte Carlo simulation but sophisticated enough to provide physically realistic dynamics. Safety analyses based on these models led to the certification of TCAS and, more recently, its worldwide mandate onboard all large transport aircraft.

The encounter models developed and described in this paper extend these prior models in several important ways. First, the models allow an arbitrary number of acceleration changes during the course of an encounter using a Markov model represented as a dynamic Bayesian network, permitting a higher-fidelity representation of what occurs in the actual airspace. Second, a more principled statistical framework for determining the parameters and structures for our models was adopted. Third, the framework was used to construct models of new categories of encounters, including encounters involving noncooperative aircraft that were not considered in prior encounter model studies.

This paper describes the encounter models developed based on surveillance data and outlines the general methodology for constructing encounter models. The encounter models presented in this paper are publicly available to support collision avoidance system development and analysis for manned and unmanned aircraft. This paper also explains how encounter models can be used to support collision avoidance safety analysis.

II. Encounter Model Overview

This section provides an overview of recent encounter models developed from 2006–2008 to evaluate TCAS and future collision avoidance systems for manned and unmanned aircraft. The next section outlines the methodology used for their construction.

Aircraft encounters can be one of two types: correlated or uncorrelated. The first type involves transponder-equipped aircraft with at least one in contact with air traffic control (ATC). It is therefore likely that both aircraft are tracked by ATC and that at least one aircraft receives some notification about the traffic conflict and begins to take action before the involvement of a collision avoidance system. This ATC intervention often leads to a correlation between the trajectories of the two aircraft that is important to include in the airspace model. Accordingly, this form of encounter is termed correlated. Prior encounter models developed for TCAS analysis were of this type. The second type of encounter involves aircraft that do not receive prior ATC notification of a conflict. Such encounters include two aircraft flying under visual flight rules (VFR) without flight-following services and encounters involving an aircraft without a transponder. In these encounters, the pilots must rely on visual acquisition or some other collision avoidance system at close range to detect each other and maintain separation. Such encounters are assumed to be uncorrelated because there is no coordinated intervention before the close encounter. Encounters of this type are especially important when evaluating collision avoidance systems for unmanned aircraft that must avoid noncooperative aircraft. The collection of encounter models described here captures both correlated and uncorrelated encounters.

To construct the models, we used a recording of real-time aircraft surveillance data streamed from the 84th Radar Evaluation Squadron (RADES) at Hill Air Force Base. The data stream encompasses both the Eastern and Western Air Defense Sectors and includes the raw sensor reports from 130 short- and long-range radars with 4.5 and 12 s update rates, amounting to approximately 10 GB of data per day. The raw reports provide range, azimuth, mode C altitude, and mode A code, from which we compute latitude and longitude coordinates and produce tracks fused from multiple sensors [9]. Figure 1 shows the number of flight hours accumulated geographically during a nine-month period. The sensors cover much of the continental United States, but there are patches in Kansas, Nebraska, and along the northwest border with Canada

a) Discrete code (IFR) traffic

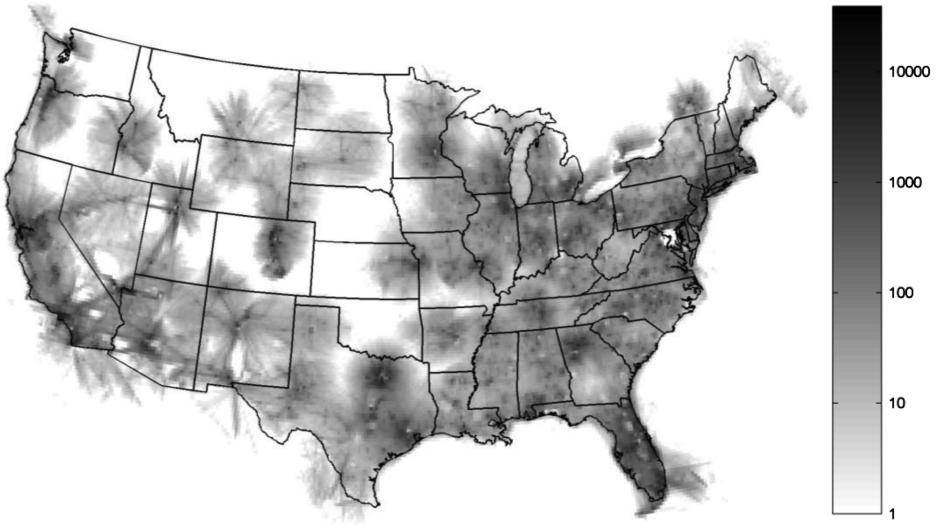

b) 1200 code (VFR) traffic

Fig. 1 Cumulative flight hours per 1/6 × 1/6 deg cell from 1 December 2007 to 31 August 2008. Cells with less than 1 flight hour of observed traffic are white.

without coverage. Because of terrain masking in some areas, lower altitudes may have limited coverage as well.

The correlated encounter model is based on encounters observed in the RADES data from 1 December 2007 to 31 August 2008. To identify encounters, we used a volume and closing rate filter similar to the one used by TCAS. To declare an encounter, the following two conditions must be met simultaneously:

$$-\frac{r - D_m}{\dot{r}} \leq T \quad \text{or} \quad r \leq D_m \tag{1}$$

$$-\frac{a}{\dot{a}} \leq T \quad \text{or} \quad a \leq Z \tag{2}$$

where r is range and a is relative altitude. The thresholds Z, D_m, and T are as defined in the TCAS Minimum Operational Performance Standard, version 6.04a [10], except that the value for Z above FL295 was reduced to 850 ft due to nuisance resolution advisories caused by the introduction of reduced vertical separation minimum. In the recorded data, 393,077 encounters involving at least one aircraft flying under instrument flight rules (IFR) were identified, many more encounters than were used to construct previous models.

The collection of encounters used to construct the correlated encounter model includes the effects of TCAS on the vertical miss distance. During the development of earlier encounter models, attempts were made to manually remove the effects of TCAS so that the model would represent nominal aircraft behavior in the absence of a collision avoidance system. Recently, an automated system was developed that leverages TCAS downlink data in deciding how to best remove the effects of advisories [11]. It was found that removing these effects from the tracks used to generate the encounter model had a negligible effect on resultant safety metrics such as the risk ratio (discussed further in Sec. V).

An uncorrelated model for conventional aircraft was created from 74,000 h of VFR flight time, as indicated by transponder code 1200. Because of the assumption that flight behavior before the encounter is uncorrelated (i.e., not affected by ATC intervention), the uncorrelated model can be based on nominal flight characteristics. Although 1200-code data can be an acceptable surrogate for a large class of noncooperative aircraft [12], we also developed nine separate uncorrelated models for various categories of unconventional aircraft, such as gliders and balloons, based on GPS flight recorder data [13]. Figure 2 illustrates the taxonomy of encounter models developed.

The general process for constructing the models from surveillance data is nearly identical for the correlated and uncorrelated models and is outlined in Fig. 3. Because surveillance data can be noisy, the first step is to preprocess the raw tracks, which involves removing outliers, smoothing, and interpolating. Outlier removal involves incrementally discarding individual reports until the magnitudes of ground speeds, turn rates, accelerations, and vertical rates are below set thresholds. The position and altitude reports are smoothed using a Gaussian kernel and interpolated to 1 Hz using piecewise cubic Hermite interpolation [9,12].

From the collection of high-quality tracks, various features defining the dynamic characteristics of the encounter are extracted, including airspeed v, airspeed acceleration $\dot{v}$, turn rate $\dot{\psi}$, and vertical rate $\dot{h}$. For the correlated encounter model, these features are extracted from both aircraft involved in an observed encounter. For the uncorrelated encounter models, these features are extracted from recorded tracks from individual aircraft. Because the dynamics of these variables are dependent upon the altitude layer L and airspace class A (e.g., an aircraft that is low and in terminal airspace is more likely to be climbing from or descending to a runway), L and A are included in the models. Because the correlated model needs to capture the geometry of the encounter induced by ATC intervention, a collection of other features are extracted. As with some previous

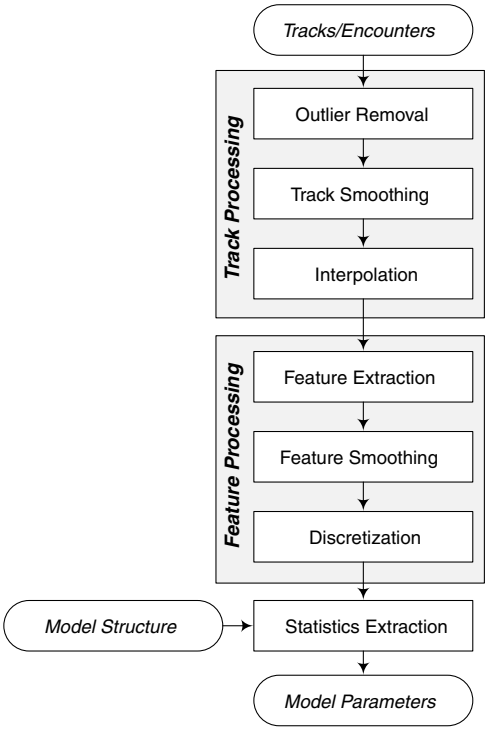

Fig. 3 General track processing sequence.

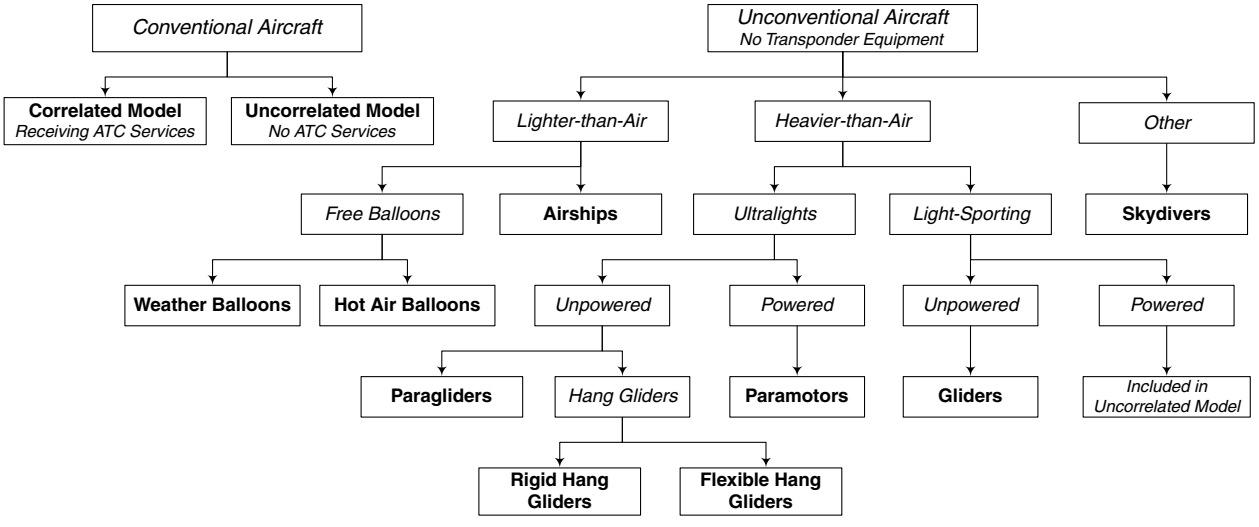

Fig. 2 Encounter model taxonomy.

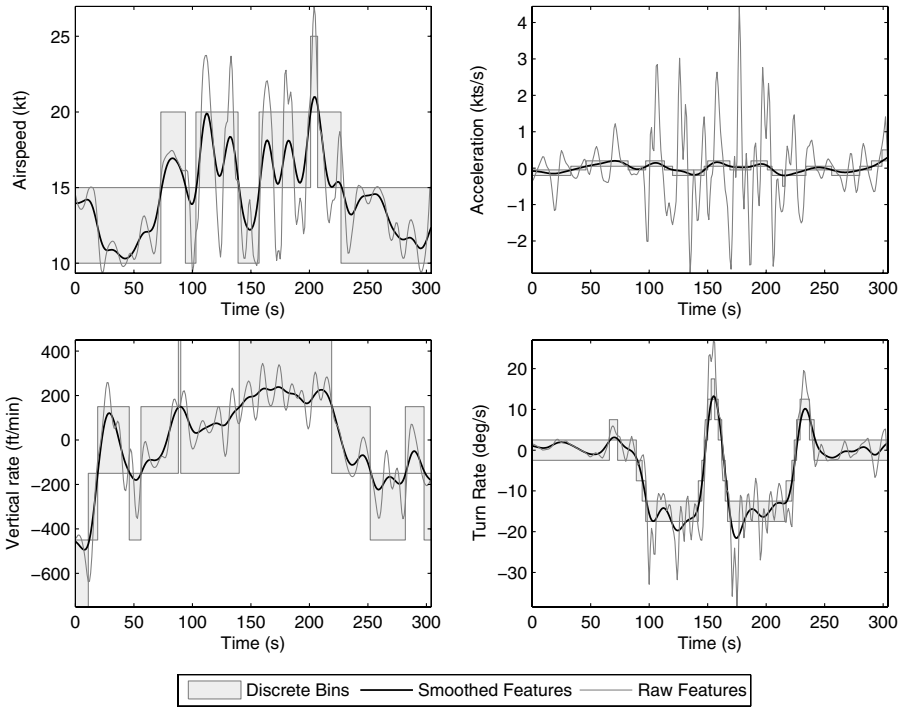

Fig. 4 Feature processing example for an ultralight track.

encounter models [5], the approach angle β, relative bearing χ, horizontal miss distance (hmd), and vertical miss distance (vmd) at the TCA are extracted. For the correlated model, we extract the categories C_1 and C_2 of the two aircraft based on whether they are squawking a discrete transponder code. Aircraft squawking a discrete code tend to maneuver less frequently than those squawking 1200, and it is important to capture this difference in flight characteristics in the model. Throughout this paper, the standard units used in aviation are used unless otherwise noted. In particular, altitudes are in feet, positions are in nautical mile coordinates, vertical rates are in feet per minute, turn rates are in degrees per second, airspeeds are in knots (true airspeed), and accelerations are in knots per second.

To remove noise, the dynamic features, such as airspeed, airspeed acceleration, vertical rate, and turn rate, are smoothed using a Gaussian kernel, as illustrated for an example track in Fig. 4. The smoothed features are then discretized into bins. The bin boundaries for the uncorrelated model of conventional aircraft are listed in Table 1. From the large set of discrete, multivariate samples, we extract statistics about the joint distribution and store them as a collection of probability tables. A methodology for representing the joint distribution, choosing its structure, and estimating its parameters is the focus of the next section.

Once the model is constructed, it may be sampled as many times as necessary for analysis. Figure 5 outlines the model sampling process. The first step in generating an encounter is to sample from the discrete probability distribution represented by the model. This results in a series of feature bins, similar to those shown in Fig. 4. We uniformly sample within the bins to create a series of continuous vertical rates, turn rates, etc., that can be used as a nominal script in a dynamic simulation.

Examples of randomly selected actual and simulated tracks are shown in Fig. 6. Although quantitative methods were used to show that the sampled features were equivalent to those observed (see Sec. IV), this figure qualitatively illustrates this comparison. Both the observed and simulated tracks exhibit similar airspeed and several turning maneuvers during this 5 min time period excerpt. The simulated track would then be geometrically paired with another track as described in Sec. V.

Table 1 Uncorrelated model bin boundaries

Variable	Units	Bin boundaries
A	——	B, C, D, and other
L	ft	500, 1200, 3000, 5000, and 12,500
v	kt	0, 30, 60, 90, 120, 140, 165, 250, and 300
$\dot{v}$	kt/s	−2, −1, −0.25, 0.25, and 1, and 2
$\dot{h}$	ft/ min	−2000, −1250, −750, −250, 250, 750, 1250, and 2000
$\dot{\psi}$	deg /s	−8, −6, −4.5, −1.5, 1.5, 4.5, 6, and 8

III. Encounter Model Construction

An encounter consists of two aircraft trajectories. Encounters with multiple aircraft are rare in the airspace, but simulating them is a straightforward extension [14]. An encounter model represents the probability distribution over the initial conditions of the encounter, such as the initial airspeed and turn rate, as well as the behavior of the aircraft over time. By running a large collection of encounters sampled from the encounter distribution, we can measure the effectiveness of a collision avoidance system when it intervenes.

After deciding which variables to model (discussed in the preceding section), the next task is to choose a representation for the probability distribution over the variables. For the naturally discrete variables, such as airspace class, we use a multinomial distribution.

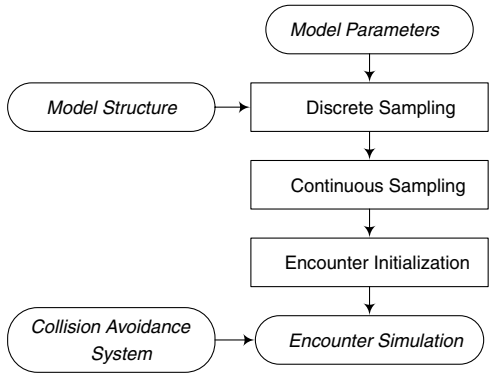

Fig. 5 Model sampling process.

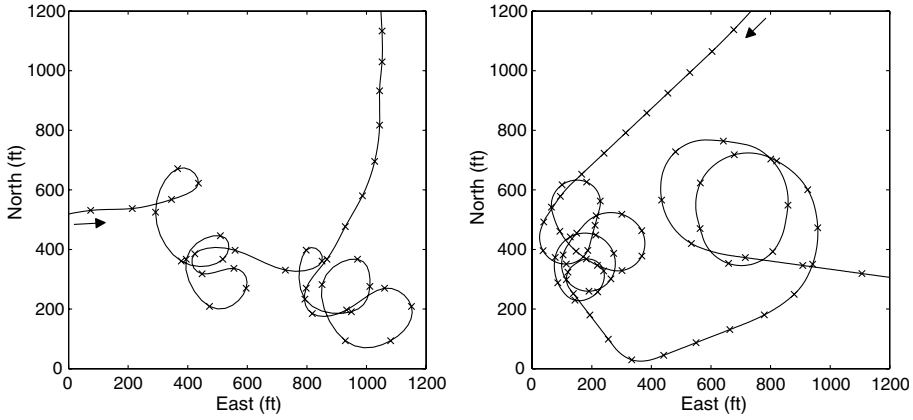

a) Example observed track b) Simulated track

Fig. 6 Observed and simulated trajectories for an ultralight. The tracks are approximately five minutes in duration. Crosses indicate 5 s intervals.

For continuous variables, such as approach angle, we discretize the variable and represent the distribution over the bins as a multinomial distribution as done in prior models. The distributions within bins are assumed to be uniform. Discretization allows us to model arbitrarily complex distributions with a sufficient number of bins.

To illustrate how we model distributions, consider the altitude layer variable in the correlated model, which can take on one of r different values. We would need r different parameters $\theta_1, \ldots, \theta_r$ to represent the multinomial distribution, where the variable is assigned value k with probability θ_k. Note that there are really only $r-1$ independent parameters because $\theta_1, \ldots, \theta_r$ must sum to 1. Suppose we have a collection of counts, $N_1, \ldots, N_r$, where N_k is a count of the number of times an encounter occurred in layer k in our radar data. The maximum likelihood estimate for θ_k is $N_k / \sum_{i=1}^{r} N_i$. Hence, if we use the maximum likelihood estimate to estimate the parameters of the distribution over altitude layer, we would produce samples from the bins with probability equal to the fraction of observed occurrences in our data set. The probability tables associated with prior encounter models were based on maximum likelihood estimates.

The maximum likelihood estimate is a sensible estimate of the true parameters, but there is uncertainty in this estimate. We can compute a distribution over the parameters $\boldsymbol{\theta} = (\theta_1, \ldots, \theta_r)$ given our data by applying Bayes' rule. It can be shown that the distribution over $\boldsymbol{\theta}$, which can be thought of as a distribution over distributions, is modeled by a special kind of distribution known as the Dirichlet distribution [15,16]. If we start with a prior distribution represented by a Dirichlet with parameters $(\alpha_1, \ldots, \alpha_r)$ and then observe the counts $N_1, \ldots, N_r$, the posterior distribution is Dirichlet with parameters $(\alpha_1 + N_1, \ldots, \alpha_r + N_r)$. A prior with all parameters set to 1 is equivalent to the belief that all possible parameter settings for $\boldsymbol{\theta}$ are equally likely. If we wanted to incorporate prior knowledge about the distribution over altitude layers, we can do this by choosing different values for $\alpha_1, \ldots, \alpha_r$. Sampling from the posterior Dirichlet distribution and then sampling from the multinomial distribution will result in assigning the variable to value k with probability

$$(\alpha_k + N_k) \Big/ \sum_{i=1}^{r} (\alpha_i + N_i)$$

which is equivalent to sampling from the maximum likelihood estimate but with $\alpha_1, \ldots, \alpha_r$ added to the observed counts. Because of the wealth of radar data, the impact of adding $\alpha_1, \ldots, \alpha_r$ to the counts is fairly insignificant in practice. However, the idea of using a Dirichlet distribution to represent our uncertainty in $\boldsymbol{\theta}$ is useful in determining how different variables in the model relate to each other, as will be discussed shortly.

The discussion so far has only addressed how to use data to estimate the distribution over a single variable independent of all others. A realistic encounter model is composed of many different variables, some of which may be related to each other. For example, airspeed is related to the altitude layer. If we know that an aircraft is flying at high altitude, it will probably be flying faster than aircraft at lower altitudes. The relationship between variables may be represented using a Bayesian network [17,18]. Two examples of graphical structures are illustrated in Fig. 7. Associated with each node is a conditional probability table that determines the probability distribution for the specified variable given the values of the variables that appear as parents in the network. The probability of an instantiation $\boldsymbol{x} = (x_1, \ldots, x_n)$ of all n variables is given by the product

$$\prod_{i=1}^{n} P(x_i | \boldsymbol{\pi}_i)$$

where $\boldsymbol{\pi}_i$ is the instantiation of the parents of the ith variable and $P(x_i|\boldsymbol{\pi}_i)$ is as given in the conditional probability tables. If the ith variable can be assigned to r_i different values (or bins) and has q_i different instantiations for its parents, then there are $r_i q_i$ probability values in its associated conditional probability table. Because the distribution must sum to 1 for a given parental instantiation, there are only $(r_i - 1)q_i$ independent probabilities for the ith variable. In total, there are

$$\sum_{i=1}^{n} (r_i - 1) q_i$$

parameters defining the conditional probability tables for a Bayesian network.

Producing a sample from a Bayesian network involves randomly assigning values to variables according to the conditional probability distributions associated with each variable. Special care must be taken when choosing the sequence of variable instantiations so that variables that depend on other (parent or ancestral) variables are instantiated after the other (parent or ancestral) variables are instantiated. More formally, we must instantiate variable i before variable j if there exists a directed path from variable i to variable j in the network. Because Bayesian networks are directed acyclic graphs, there will always exist at least one such ordering, called a topological sort, and efficient algorithms exist for topological sorting [19]. The first variable in the topological sort gets instantiated randomly according to its associated probability distribution table. Later variables in the sort get instantiated randomly according to their associated conditional probability tables, which may depend upon variables that were instantiated earlier.

The value of a Bayesian network is that it leverages conditional independence between variables to reduce the number of parameters required to define the joint distribution over the variables. Directly defining the probability of every possible instantiation of the variables would require

$$\prod_{i=1}^{N} r_i - 1$$

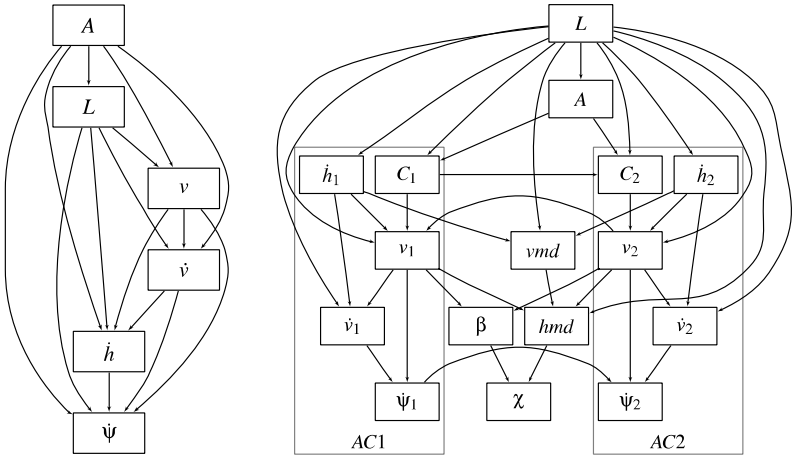

a) Uncorrelated model b) Correlated model

Fig. 7 Initial Bayesian network structure: shown are the variables used in the models to represent the encounter geometry between two aircraft and their initial state.

parameters, which scales exponentially with the number of variables. To illustrate the savings, it requires 17,358 parameters to define the Bayesian network in Fig. 7a compared to more than 400 billion parameters when defining the joint distribution directly. The problem with models with many parameters is that they require a large amount of data to estimate them well.

The structure of prior encounter models may be thought of as Bayesian networks, although they are not described as such in their documentation. In prior encounter models, the structure was decided upon using engineering judgment without detailed analysis of the statistical properties of the data. Choosing the best network structure is difficult. Omitting important correlations between variables will result in the generation of unrealistic encounters, but adding too many directed arcs to a Bayesian network results in an unnecessary growth in the number of parameters and wastes data. Using statistical techniques developed since the mid-1990s in the machine learning community [20,21], we can infer the structure of the model from the data. These techniques involve searching through the space of network structures for the network that has the greatest posterior probability. In other words, they look for the graph G that maximizes $P(G|D)$, where D is the data. From Bayes' rule, we know $P(G|D)$ is proportional to $P(G)P(D|G)$. The prior belief over the space of graphical structure $P(G)$ may be used to encode an engineer's preference over the graphical structures before observing any data; otherwise, $P(G)$ can be treated as uniform. The likelihood $P(D|G)$ is computed by integrating over the uncertainty in the conditional probability tables as represented by a collection of Dirichlet distributions. Cooper and Herskovits [22] show how to perform this integration:

$$P(D|G) = \int P(D|\boldsymbol{\theta}, G)\, p(\boldsymbol{\theta}|G)\, \mathrm{d}\boldsymbol{\theta} = \prod_{i=1}^{n} \prod_{j=1}^{q_i} \frac{\Gamma(\alpha_{ij})}{\Gamma(\alpha_{ij} + N_{ij})} \prod_{k=1}^{r_i} \frac{\Gamma(\alpha_{ijk} + N_{ijk})}{\Gamma(\alpha_{ijk})} \tag{3}$$

Here, N_{ijk} is the count of the number of times the ith variable took on its kth value when the values of its parents corresponded to their jth collective instantiation. The Dirichlet prior used for the distribution of the ith variable given the jth parental instantiation uses parameters $(\alpha_{ij1}, \ldots, \alpha_{ijr_i})$. In Eq. (3),

$$\alpha_{ij} = \sum_{k=1}^{r_i} \alpha_{ijk}$$

and

$$N_{ij} = \sum_{k=1}^{r_i} N_{ijk}$$

In practice, it is not practical to evaluate $P(G|D)$ on every possible graphical structure and it is known that, in general, finding the network with the greatest $P(G|D)$ is NP-complete [23]. Hence, a variety of heuristic search methods have been suggested in the machine learning literature [16,24]. Before settling upon the structures of our encounter models, we used a variety of heuristic search methods implemented in the GeNIe modeling environment developed by the Decision Systems Laboratory at the University of Pittsburgh.

We have described how to use a Bayesian network to model a joint distribution over static variables, such as the altitude layer and the airspeed at the beginning of an encounter. Many of the variables in the encounter model need to change over time to capture the dynamics of real encounters. Prior encounter models had additional static variables that determine the start and end times of maneuvers and the strength of the maneuver. The disadvantage of this approach is that it only allows single acceleration periods. Of course, additional variables for the start and end times of additional maneuvers could be incorporated but doing so would significantly increase the complexity of the model.

We used a special kind of Bayesian network called a dynamic Bayesian network [25,26] to represent the dynamics of the variables (see Fig. 8). A dynamic Bayesian network is composed of two slices: the first slice represents the values of variables at time t and the second slice represents the values of variables at time $t + 1$. To create an encounter trajectory, we sample from a static Bayesian network to get the initial values of the variables and then use a dynamic Bayesian network to propagate the trajectories. At the first time step, the initial values obtained by sampling the static Bayesian network are held

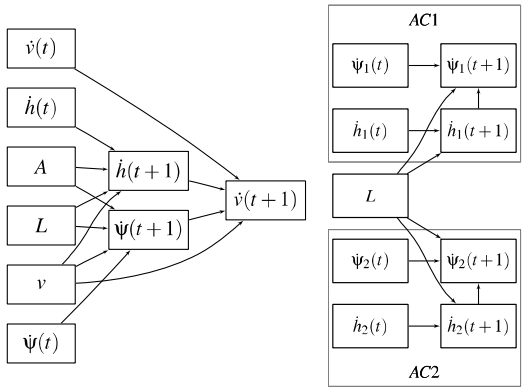

a) Uncorrelated model b) Correlated model

Fig. 8 Dynamic Bayesian networks: shown are the variables used in the model to represent how the behavior of the aircraft involved in the encounter evolve over time.

fixed and the variables at time $t+1$ are sampled. The newly sampled values are then held fixed and new values are sampled for the next time step. The process is repeated as long as necessary.

The assumption behind our Bayesian network is that the next state of the system depends only upon the current state. This is known as the Markov assumption, and many dynamic systems that hold to this assumption have been studied in the literature. If a system is non-Markovian, then additional slices can be added to the dynamic Bayesian network or additional variables can be added to the model [26]. We validated our model by comparing a set of sample encounters generated by our model against observed encounters using features not included in our model and found that our dynamic Bayesian network adequately captured the important characteristics of real encounters [9].

IV. Model Validation

The correlated and uncorrelated models, and the method for which they are sampled and used in a dynamic simulation, must be representative of the encounters and aircraft for which they were intended. It is important to have confidence that the generated samples are characteristic of the encounters and aircraft in the airspace. In addition, the dynamic simulation must provide realistic encounters. This can be quantified by comparing the encounter and aircraft characteristics that were not modeled explicitly to those that were observed. These validation steps are described in this section.

A. Sampling Validation

The basic step in model validation is verifying the implementation of the sampling scheme. To verify the sampling scheme, we generated a large collection of samples, collected the feature distributions as was done to compile the models, and compared them to the observed features distributions. We began by verifying that the marginal distributions closely match by comparing histograms for the model variables. To validate that the correlations between variables in the generated encounters match the observed encounters, one may compute $P(\boldsymbol{\theta}_1 = \boldsymbol{\theta}_2 | D_1, D_2)$, where D_1 and D_2 represent the data associated with the observed features and sampled features and $\boldsymbol{\theta}_1$ and $\boldsymbol{\theta}_2$ represent the model parameters. If the sampling was implemented correctly, this probability should be close to 1. Applying Bayes' rule results in

$$P(\boldsymbol{\theta}_1 = \boldsymbol{\theta}_2 | D_1, D_2) = \frac{P(\boldsymbol{\theta}_1 = \boldsymbol{\theta}_2) P(D_1, D_2 | \boldsymbol{\theta}_1 = \boldsymbol{\theta}_2)}{P(D_1, D_2)} \tag{4}$$

which is the prior $P(\boldsymbol{\theta}_1 = \boldsymbol{\theta}_2)$ times the ratio

$$\frac{\int P(D_1, D_2 | \boldsymbol{\theta}) p(\boldsymbol{\theta}) \, \mathrm{d}\boldsymbol{\theta}}{\int P(D_1 | \boldsymbol{\theta}) p(\boldsymbol{\theta}) \, \mathrm{d}\boldsymbol{\theta} \int P(D_2 | \boldsymbol{\theta}) p(\boldsymbol{\theta}) \, \mathrm{d}\boldsymbol{\theta}} \tag{5}$$

Defining $f(D) = \int P(D|\boldsymbol{\theta}) p(\boldsymbol{\theta}) \, \mathrm{d}\boldsymbol{\theta}$, the ratio becomes $f(D_1 \cup D_2)/(f(D_1) f(D_2))$. The greater this ratio, the more likely the distributions are the same. Using the uncorrelated model with 1000 samples, the base 10 log ratio was 1.4×10^3 for the initial network and 1.5×10^3 for the dynamic network, indicating with high confidence that the samples came from the same distribution as the model.

B. Dynamic Simulation Validation

Comparing variables not included in the model to those extracted from the dynamic simulation is one metric for ensuring that the simulated encounters are representative of the variation in the airspace. A previous Eurocontrol correlated model explicitly captured the number of altitude crossing encounters [5]. In our recorded radar data, 12.5% of the encounters were crossing, whereas 11.42% of the simulated encounters were crossing. Similarly, we examined the rate of slow-closing encounters, or encounters that begin at a close range 40 s before TCA. Approximately 0.34% of actual encounters were observed to be slow-closing encounters and of the 10,000 randomly generated samples, 0.56% were slow-closing encounters. These results suggest that the model is successful at producing encounters that are realistic and reflect what occurs in the airspace.

The validity of the uncorrelated dynamic model was assessed by comparing simulated airspeed to that observed. Although initial airspeed is sampled from the model specifying the initial conditions, it is propagated through time using sampled acceleration. Thus, it is possible that airspeed is propagated to an unobserved value if left unbounded, no longer reflecting the observed distribution of airspeed. The marginal airspeed distribution at each time step for 100,000 tracks over 600 s was compared using a modified parametric χ^2 goodness-of-fit test, which was assumed independent of sample size. Assuming a p-value threshold of 1%, the uncorrelated model was deduced valid for approximately 103 s, which meets the baseline requirement of 60 s. There may be instances where a longer track length may be needed (e.g., multiple intruder encounters). One method for increasing the validity time of the model is to reject samples whose airspeeds exceed the observed limits at any point in the trajectory. This rejection process increases the validity length to 195 s for the uncorrelated model.

As additional validation for the uncorrelated model sampling scheme and dynamic simulation, we compared the density of 100,000 randomly selected actual 1200-code radar segments 60 s in length to those sampled from the model. The trajectories were selected and generated, through rejection sampling, to have initial airspeed $v \in [90, 120)$, turn rate $\dot{\psi} \in [-1.5, 1.5)$ and vertical rate $\dot{h} \in [-250, 250)$. Initial position and heading were set to zero while initial acceleration, airspace class, and altitude layer were unconstrained. Figure 9 shows the position densities at 15 and 30 s intervals. The nominal trajectory, or the track with the maximum likelihood, is superimposed for reference. Two sampling schemes are shown: 1) assuming a uniform distribution (see Fig. 9b and 9e) for the bin encompassing zero for vertical rate, acceleration, and turn rate; and 2) rounding to zero all sampled values within the bins that include zero (see Fig. 9c and 9f). The second case assumes that aircraft are not actually maneuvering when small maneuvers are observed. These plots show that the spatial bounds are similar and that the radar distribution shares attributes of both the uniform and rounding sampling schemes. This second characteristic is caused by the continuous feature distribution peak not being correctly described by either sampling scheme. The uniform scheme results in higher diffuseness than the radar density, whereas the rounding scheme results in greater clustering along the zero turn rate, or due north, path. If a closer match is desired, the sampling scheme could be modified by using a nonuniform distribution that better fits the observed peak or by introducing additional bins.

V. Safety Analysis

Encounter models are used in simulations to estimate the probability that an encounter leads to a near-midair collision (NMAC), which has been defined in prior TCAS studies as being a loss of separation 100 ft vertically and 500 ft horizontally. Estimating NMACs is easier than estimating actual midair collisions because, among other reasons, knowledge about the airframes involved in the encounter is unnecessary. Historically, it has been assumed that approximately 10% of NMACs result in collisions [27].

To estimate NMAC rate, we simply multiply the encounter rate by the probability an encounter leads to an NMAC. The encounter rate may be estimated from radar data. However, many safety studies are primarily concerned with estimating the risk ratio, which is the NMAC rate with the collision avoidance system divided by the NMAC rate without the system. Because the encounter rate is assumed to be independent of collision avoidance equipage, risk ratio reduces to the probability an encounter leads to an NMAC with the system divided by the probability an encounter leads to an NMAC without the system.

To estimate the probability an encounter leads to an NMAC, we generate a large collection of encounters using an encounter model and run them in simulation. Dividing the number of encounters that lead to an NMAC by the total number of encounters run in simulation provides a Monte Carlo estimate of $P(\text{nmac}|\text{enc})$. The remainder of

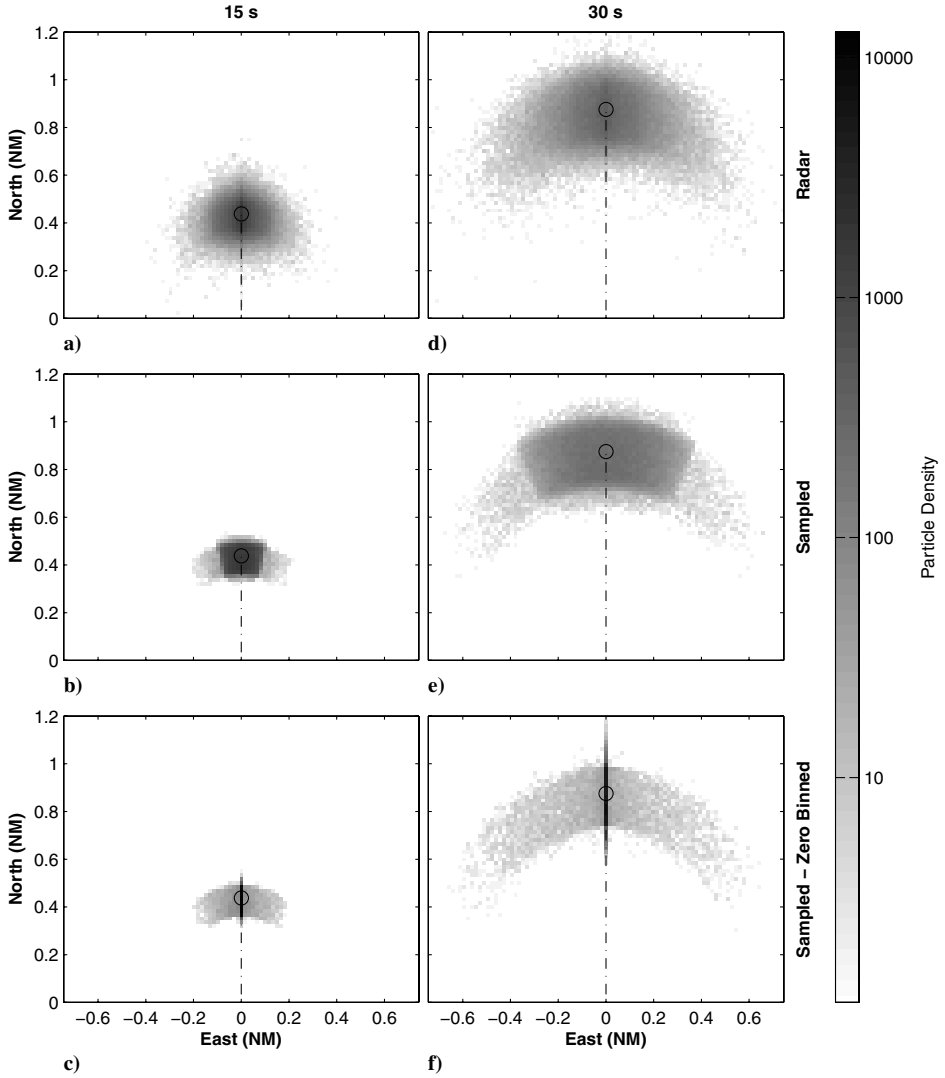

Fig. 9 Qualitative comparison of 1200-code radar tracks to sampled tracks from the uncorrelated model.

this section explains how we go about estimating $P(\text{nmac}|\text{enc})$ using correlated and uncorrelated models.

A. Estimating Probability of NMAC Using a Correlated Model

The first step in generating an encounter involves sampling from the initial network (see Fig. 7b), which provides the initial values of the dynamic variables, such as the vertical rate and turn rate for both aircraft. The initial network also provides the geometry at the TCA, including the approach angle, relative bearing, vertical miss distance, and horizontal miss distance. Using the initial values of the dynamic variables obtained from the initial network, the dynamic network (see Fig. 8b) propagates the trajectories by generating the values of the dynamic variables over time.

We convert the sequence of turn rates, vertical rates, etc., generated by our model into trajectories in three-dimensional space. We then rotate and translate the aircraft trajectories so that the geometry at TCA matches what was sampled. The initial positions of the aircraft after transformation are used as the initial positions when simulating the encounters. If the collision avoidance system detects a threat during the course of the encounter, it will deviate at some point from the nominal path.

Directly sampling from the Bayesian network and computing the average number of NMACs will provide an unbiased estimate of the probability that an encounter results in an NMAC. However, because of the rarity of NMAC events in the airspace, direct sampling from the encounter distribution will result in the generation of relatively few NMACs. Simulating encounters that are unlikely to result in an NMAC is inefficient. Instead, we want to produce encounters that have mostly low vertical and horizontal separation at TCA and then weight the encounters appropriately. Such an approach is known as importance sampling and has been widely studied in the literature as a variance-reduction technique in estimation [28]. An approach similar to importance sampling was used in prior encounter models.

More formally, a direct sampling approach produces a collection of N encounters $z^{(1)}, \ldots, z^{(N)}$ from the probability distribution $p(z)$ represented by the encounter model, permitting the following approximation:

$$P(\text{nmac}|\text{enc}) = \int P(\text{nmac}|z)p(z)\,\mathrm{d}z \approx \frac{1}{N}\sum_{i=1}^{N} P(\text{nmac}|z^{(i)}) \quad (6)$$

The probability $P(\text{nmac}|z^{(i)})$ is evaluated through simulation. In importance sampling, the samples $z^{(1)}, \ldots, z^{(N)}$ are chosen according to an alternative distribution $q(z)$. The approximation becomes

$$\begin{aligned} P(\text{nmac}|\text{enc}) &= \int P(\text{nmac}|z)p(z)\frac{q(z)}{q(z)}\,\mathrm{d}z \\ &= \int P(\text{nmac}|z)q(z)\frac{p(z)}{q(z)}\,\mathrm{d}z \approx \frac{1}{N}\sum_{i=1}^{N} P(\text{nmac}|z^{(i)})\frac{p(z^{(i)})}{q(z^{(i)})} \end{aligned} \quad (7)$$

The factor $p(z^{(i)})/q(z^{(i)})$, as can be seen in Eq. (7), is used to weight the result of encounter $z^{(i)}$ in simulation.

The strategy in importance sampling is to choose $q(z)$ to be as proportional to $P(\text{nmac}|z)p(z)$ as possible [29]. Because the horizontal and vertical miss distance of the nominal flight paths at TCA most significantly influence whether the encounter results in an NMAC, we focused the distribution $q(z)$ on low horizontal and vertical miss distances. We sample from $q(z)$ by sampling from our encounter model and then overwriting the horizontal and vertical miss distance variables using values selected independently from distributions $q(\text{hmd})$ and $q(\text{vmd})$. We chose $q(\text{hmd})$ to produce horizontal miss distances of less of than 500 ft with probability 0.95, and we chose $q(\text{vmd})$ to produce vertical miss distance of less than 100 ft approximately half of the time. It is important to select some horizontal and vertical miss distances that are larger than the NMAC definition to capture potential NMACs induced by the collision avoidance system. The weight $p(z^{(i)})/q(z^{(i)})$ is equal to

$$\frac{p(\text{hmd}^{(i)}|\pi_{\text{hmd}}^{(i)})p(\text{vmd}^{(i)}|\pi_{\text{vmd}}^{(i)})}{q(\text{hmd}^{(i)})q(\text{vmd}^{(i)})} \tag{8}$$

The value of the parents of hmd and vmd are denoted $\pi_{\text{hmd}}^{(i)}$ and $\pi_{\text{vmd}}^{(i)}$ respectively, and the probabilities $p(\text{hmd}^{(i)}|\pi_{\text{hmd}}^{(i)})$ and $p(\text{vmd}^{(i)}|\pi_{\text{vmd}}^{(i)})$ are obtained from the conditional probability tables associated with the Bayesian network. Importance sampling results in faster convergence of the $P(\text{nmac}|\text{enc})$ estimate. Hence, fewer samples are required to obtain the same accuracy in the estimate compared to direct sampling.

B. Estimating Probability of NMAC Using an Uncorrelated Model

The concept behind the uncorrelated model is that an aircraft, whose collision avoidance system we wish to evaluate, travels through the airspace with some large encounter cylinder fixed to its center, and the intruder aircraft is initialized on the cylinder. The appropriate dimensions of the encounter cylinder depend on the aircraft dynamics and collision avoidance system. If the encounter cylinder is too small, the collision avoidance system will not have sufficient opportunity to be fully exercised before a collision. If the encounter cylinder is too large, then computation is wasted. We can choose the dimensions of the cylinder by multiplying the magnitude of the maximum expected closure rate by the approximate time required by the collision avoidance system to detect and avoid an intruder. If we assume that the density of air traffic outside the cylinder is uniform in the local region being studied and the trajectories of the aircraft outside the cylinder are independent of the own aircraft, then there is no need to waste simulation time modeling the air traffic outside the cylinder. Instead, simulation can focus on the behavior of intruder aircraft after penetrating the cylinder. To estimate the NMAC rate, we multiply the rate at which aircraft penetrate the cylinder by the probability that an aircraft that penetrates the cylinder results in an NMAC before exiting the encounter cylinder: $P(\text{nmac}|\text{enc})$.

In contrast with the correlated model, the nominal trajectories of the aircraft involved in the encounter are modeled independently. To model different intruder types, including conventional VFR aircraft, gliders, and balloons (see Fig. 2), we constructed a collection of Bayesian networks based on radar and flight recorder data. The nominal path of the aircraft whose collision avoidance system we want to evaluate can be generated from the intended flight plan, recorded surveillance data, or some dynamic model.

As with the correlated encounter model, $P(\text{nmac}|\text{enc})$ can be estimated using a Monte Carlo approach. Unfortunately, we cannot simply divide the number of sampled encounters that lead to NMACs by the total number of sampled encounters to estimate $P(\text{nmac}|\text{enc})$ because of the fact that sampling from the uncorrelated model Bayesian networks does not produce encounters from the same distribution that would occur in the airspace. In particular, the Bayesian networks generate encounters with aircraft velocities distributed identically to the aircraft population at large, despite the fact that in reality the distribution of aircraft velocities given that an encounter is occurring favors high-speed aircraft. Although we sample from a distribution that is different from the true distribution when constructing encounters, we can still use the samples to estimate $P(\text{nmac}|\text{enc})$ as long as we weight their results properly as we did when using importance sampling in the correlated model. The weight of a sample is a function of the mean flux of intruders through the encounter cylinder with the sampled initial ground speed and vertical rate. The derivation of the weighting scheme is provided elsewhere [30] and the calculation of mean flux is based on work by May [31].

The rate at which aircraft penetrate the cylinder is equal to average traffic density times the mean flux of intruder aircraft through the encounter cylinder. Traffic density may be estimated from radar surveillance. Because density varies significantly over the airspace, it is important to estimate density based only on the regions and altitude layers that are of interest. Monte Carlo simulation can provide an estimate of the mean flux of intruder aircraft through the encounter cylinder [30].

The overall uncorrelated NMAC rate, encompassing all aircraft categories, is simply the sum of the NMAC rates for each intruder category. Computing NMAC rate for a particular intruder category requires knowing traffic density, which may be obtained through primary and secondary radar surveillance. One of the challenges in estimating the density of different aircraft categories is classifying the radar tracks into the 10 different model categories (as shown in Fig. 2). One approach is to create a Bayesian classifier, where the class-conditional distributions are given by the Bayesian networks associated with the models [32]. If $\omega_1, \ldots, \omega_n$ is our collection of models and $\boldsymbol{x}$ is our observed track, the posterior probability $P(\omega_i|\boldsymbol{x})$ is proportional to $P(\omega_i)P(\boldsymbol{x}|\omega_i)$. The prior $P(\omega_i)$ reflects how often we expect to see aircraft belonging to category ω_i before observing any data. The likelihood $P(\boldsymbol{x}|\omega_i)$ is provided directly from the static and dynamic Bayesian networks associated with model ω_i. Classifying $\boldsymbol{x}$ as belonging to the class whose posterior is greatest will minimize the rate of misclassification.

VI. Application Examples

In this section, we present examples of safety analyses of collision avoidance systems performed using the encounter models described in this paper. The first is an analysis of the safety benefit associated with upgrading from the current TCAS version 7.0 to a newer proposed version 7.1. The second example shows an estimate of the NMAC rate between an unmanned aircraft and noncooperative traffic for a prototype collision avoidance algorithm being developed for a high-altitude long-endurance (HALE) unmanned aircraft. The third example shows how the encounter model can be used to predict the future position of intruder aircraft.

A. TCAS

TCAS is mandated on larger transport aircraft in the United States and worldwide. The most recently mandated version of TCAS is 7.0 [3,33]. As a result of recent monitoring and modeling efforts, several change proposals have been implemented to create version 7.1 of the TCAS logic [34]. One change addresses a safety issue with preventing or delaying a reversal in the vertical sense of the avoidance maneuver that might otherwise improve aircraft separation in degrading conditions [27]. It is believed that this issue was a factor in several recent events, including two accidents: an NMAC in Japanese airspace between a B-747 and a DC-10-40 on 31 January 2001 (resulting in injuries), and the midair collision between a B-757 and a Tu-154 over Überlingen, Germany, on 1 July 2002. A second change rectifies observed confusion surrounding the aural annunciation "Adjust vertical speed, adjust" during a resolution advisory by replacing it with the annunciation "Level off, level off."

Using the correlated encounter model and the importance sampling scheme described in Sec. V.A, we generated 500,000 correlated encounters to analyze TCAS. We then simulated encounters using a fast-time simulation [35] implemented on a parallel computing environment to estimate $P(\text{nmac}|\text{enc})$ [36]. Each encounter is simulated with TCAS version 7.0 or 7.1 against intruders equipped or not equipped with TCAS. To model the pilot response to the TCAS

Table 2 Simulation results for TCAS

TCAS version on ownship	Intruder equipage	Intruder pilot response model	P(nmac|enc)	Error (standard deviation)	Risk ratio
Unequipped	Unequipped	——	3.1×10^{-3}	3.2×10^{-5}	1
7.0	TCAS version 7.0	ICAO standard	5.0×10^{-5}	5.7×10^{-6}	0.016
7.0	TCAS version 7.0	None	3.1×10^{-4}	3.0×10^{-6}	0.099
7.0	Unequipped	——	4.0×10^{-4}	7.6×10^{-6}	0.125
7.1	TCAS version 7.1	ICAO standard	4.9×10^{-5}	5.7×10^{-6}	0.016
7.1	TCAS version 7.1	——	3.0×10^{-4}	3.0×10^{-6}	0.096
7.1	Unequipped	None	3.9×10^{-4}	7.6×10^{-6}	0.123

resolution advisory, we used the standard International Civil Aviation Organization (ICAO) pilot response model, which assumes a vertical acceleration of one-quarter of the acceleration of gravity 5 s after the resolution advisory is issued [4]. We also modeled encounters where the pilot of the intruder aircraft does not respond to its TCAS resolution advisory.

Table 2 summarizes the simulation results and reports the jackknife estimates of the error [37]. The baseline P(nmac|enc) without any collision avoidance action is approximately 0.0031. With TCAS advisories and pilot response, these probabilities were reduced by a factor of approximately eight to 50 (risk ratios between 0.016 and 0.12) depending on the specific equipage and pilot responses assumed in the simulations. In every equipage and pilot response combination simulated, TCAS version 7.1 lowered the risk of NMAC compared to TCAS version 7.0. Additional safety metrics support the same conclusion that more risk lies in remaining with the status quo (7.0) over upgrading (7.1). Upgrading to TCAS version 7.1 provides the greatest safety benefit over version 7.0 when one pilot does not respond to his or her TCAS resolution advisory. Because it is well known that pilots do not always respond to their advisories [27], this result is particularly important in justifying the upgrade to TCAS version 7.1.

Recorded surveillance data indicate that the encounter rate for IFR aircraft averaged over the entire United States is approximately 0.0163 encounters per flight hour, or one encounter every 61.3 flight hours [9]. Based on this value and our simulation results, the baseline rate of NMACs for IFR aircraft without TCAS in the United States is 5.05×10^{-5} NMACs per flight hour. Assuming all aircraft are equipped with TCAS version 7.1 and responded to their TCAS resolution advisories the rate of NMACs becomes 8.13×10^{-7} NMACs per flight hour. Further details of this study may be found in a technical report [38].

B. Collision Avoidance for HALE Unmanned Aircraft

Collision avoidance systems for unmanned aircraft will have to demonstrate the ability to avoid noncooperative traffic, as well as cooperative traffic because unmanned aircraft do not have a pilot in the cockpit to accept responsibility for visually acquiring and maintaining separation [39–44]. We used the uncorrelated encounter model to evaluate a prototype collision avoidance system for a HALE unmanned aircraft. We generated one million encounters between a HALE unmanned aircraft and a noncooperative intruder to evaluate the prototype system with an encounter cylinder height of ± 2500 ft and a radius of 5 n mile. An encounter cylinder of this size ensures that the collision avoidance system has at least 30 s to track and maneuver to avoid an intruder aircraft. The encounter cylinder dimensions are large enough to ensure that the collision avoidance system being studied has sufficient time to track and avoid the intruder aircraft. Making the cylinder larger wastes computation.

The process to initialize encounters with the uncorrelated encounter model assumes that aircraft in the airspace are uniformly distributed (i.e., the position and heading of all aircraft) outside of the encounter cylinder and that aircraft randomly blunder into each other. The probability that an intruder is anywhere on the cylinder is equally likely; whether the intruder penetrates the encounter cylinder is a function of the aircraft relative airspeed and heading. This initialization process results in more intruders initialized on the front of the cylinder because that is the direction of the unmanned aircraft initial velocity vector. Figure 10 shows the initial bearing distribution of intruder aircraft that are initialized on the side of the encounter cylinder. The generated encounters emphasized situations where the HALE is climbing or descending because a HALE unmanned aircraft is most likely to encounter traffic when climbing from takeoff to its operational altitude or descending to land.

Table 3 presents simulation results for the prototype system and shows that the risk ratio for the prototype system is 0.193. That is, for every five NMACs that occur without the system, approximately one occurs with the system. Table 3 separates the results for the system by unresolved and induced NMACs. An unresolved NMAC is one that occurs both with and without the system and an induced NMAC is one that occurs with the system but not without the system. Comparing the relative rates that unresolved and induced NMACs occur can reveal operational characteristics of the system. The prototype system studied here is very successful at resolving NMACs that would occur without the system; it resolved approximately 97% of NMACs that otherwise would occur. However, approximately 85% of the NMACs that occur with the prototype system are induced. Further investigation revealed that the system reliably detects threatening aircraft but that it also has difficulties rejecting nonthreatening aircraft and maneuvers frequently, resulting in induced NMACs.

Further analysis of the system in Fig. 11 shows that this prototype system, as with TCAS [27], has the most difficulty in the lowest altitude layer of the uncorrelated model, which is where intruder aircraft are most likely to be maneuvering (e.g., turning, varying their turn rate, climbing, and descending). Results from simulations using the uncorrelated model indicate that improvement in the prototype system performance can be achieved by enhancing its ability to project the trajectories of turning intruders. This outcome suggests that an encounter model can be used to iteratively improve the collision avoidance system in addition to assessing its safety performance. Caution must be taken to ensure that the collision avoidance system parameters are not overly tuned such that a change to the airspace would unacceptably degrade system safety.

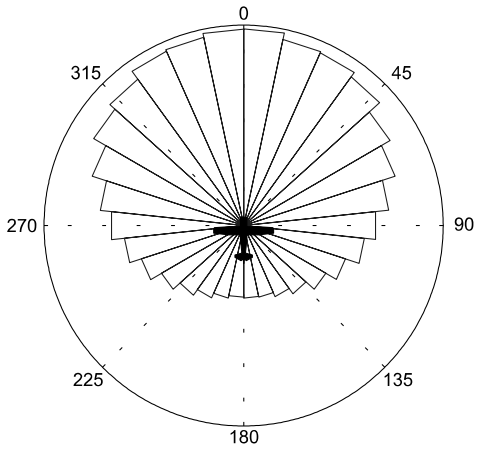

Fig. 10 Bearing distribution of intruder aircraft.

Table 3 Simulation results for prototype HALE collision avoidance system

	Without prototype system	With prototype system	Risk ratio
P(unresolved nmac|enc)	n/a	0.000012	0.0283
P(induced nmac|enc)	——	0.000070	0.165
Overall P(nmac|enc)	0.00424	0.000082	0.193

C. Probabilistic Intruder Trajectory Estimation Model

Accurately predicting the trajectory of an intruder aircraft is essential to a collision avoidance system. There are three general approaches to aircraft state extrapolation in the literature: nominal, worst case, and probabilistic [45]. The strength of a probabilistic approach is that it accounts for uncertainty in aircraft behavior and tends to be neither overly optimistic (as with nominal projection) nor overly pessimistic (as with worst case projection). Several probabilistic approaches that use parametric error models [46,47] and Monte Carlo simulation [48,49] have been examined in the literature. The success of these extrapolation methods depend upon the accuracy of the model. A model that captures turn rate, vertical rate, and airspeed dynamics and is based on actual radar data is likely to provide better predictions than the simplistic Gaussian error models typically used in the literature.

Figure 9 provided examples of projections of intruder aircraft using the uncorrelated model. Figure 12 further illustrates how the uncorrelated conventional model can be used to predict the position of an aircraft that is initially flying level at an example 105 kt with a 3 deg turn rate. The plot shows the lateral position of 100,000 samples taken from the dynamic Bayesian network 15 and 30 s into the future. The plot shows that the turn rate of an aircraft already in a turn will typically decrease with time, unlike the straight and level case shown in Fig. 9, where the spatial distribution about the nominal path is nearly symmetric (i.e., the likelihood of the aircraft turning in either direction is the same).

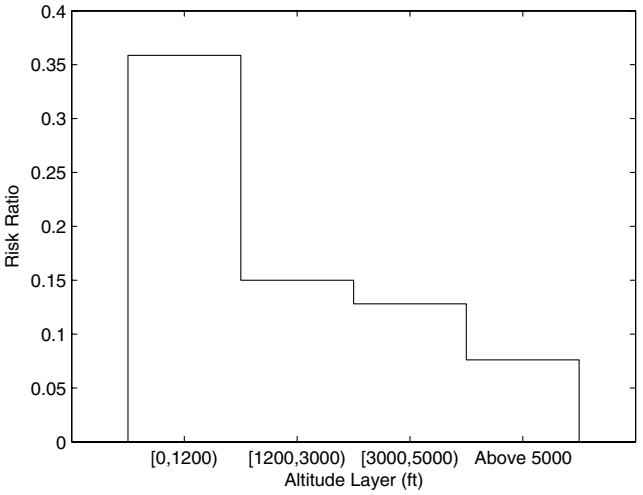

Fig. 11 Prototype system risk ratio as a function of altitude layer.

In addition to enhancing future state prediction, the encounter models can be used to improve aircraft state estimation and filtering. The dynamic model can be used directly as the process noise model in applications, where a process noise model can be non-Gaussian (e.g., particle filtering methods [50]). A time-varying Gaussian approximation to the dynamic distributions may be used when a Gaussian noise model is assumed.

D. Additional Applications

The encounter models may also be used to develop sensor requirements for unmanned aircraft. An ideal electro-optical onboard sensor for detecting intruder aircraft, for example, would provide 4π sr of coverage about the unmanned aircraft [51]. However, equipping an unmanned aircraft with enough cameras to provide full coverage is likely to be costly or infeasible. The encounter models can be used evaluate the relative performance of different sensor field-of-view configurations in terms of probability of detection before near miss [52]. The encounter models have also been used directly in the development of a hazard-alerting system based on target line-of-sight rate [53].

VII. Conclusions

This paper introduced an analytic framework and methodology for encounter modeling and collision risk estimation. To better represent observed encounters in the radar data and overcome the limitation of previous models to encounters with limited maneuvering, dynamic Bayesian networks were used to represent airspeed, turn-rate, and vertical-rate changes. The model parameters and structure are inferred from recorded data, borrowing theory originally developed in the machine learning literature for Bayesian networks. The methodology presented in this paper was used to create a collection of encounter models for different categories of conventional and unconventional aircraft. The encounter models are publicly available to support collision avoidance system safety analysis.

The nature of the airspace will change significantly over the next 20 years with the introduction of new procedures and technologies. These changes will likely affect the way in which aircraft encounter each other, making future updates to the encounter models important. The analytical framework outlined in this paper can serve as a basis for future encounter model development and collision risk assessment.

In the past, encounter models have been used to evaluate collision avoidance systems, such as the Traffic Alert and Collision Avoidance System, that have been carefully engineered and manually tuned. An automated process for constructing collision avoidance logic based on probabilistic airspace models is appealing because of the potential to significantly reduce development time and costs. One approach

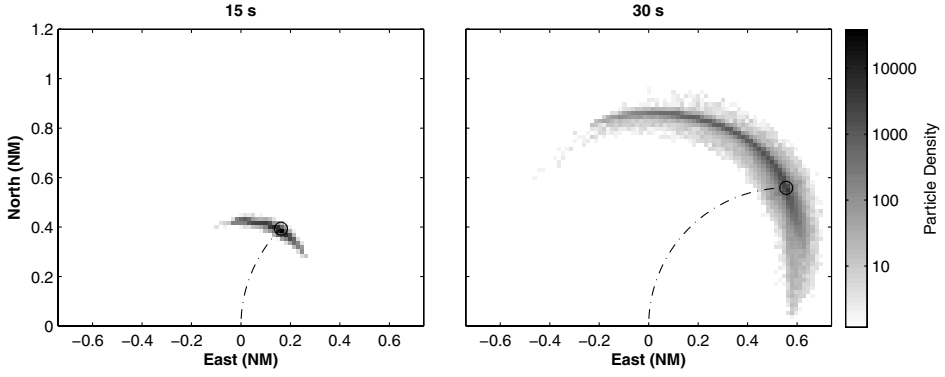

Fig. 12 Example of constrained initial conditions propagated with the uncorrelated conventional dynamic model. The dashed line indicates the nominal path.

that is currently being investigated, both for sense-and-avoid systems for unmanned aircraft and next-generation TCAS, is the formulation of the collision avoidance problem as a partially observable Markov decision process (POMDP). The state dynamics of the POMDP are derived from the encounter model and the observation model is derived from sensor specifications. Automated POMDP solvers search for avoidance policies that minimize the expected costs of collision and maneuvering. Changes to the encounter model and sensor specifications will require resolving for the optimal avoidance policy but would require far less human effort than manually retuning the collision avoidance system [54].

Acknowledgments

This work is sponsored by the U.S. Air Force, Department of Homeland Security, and Federal Aviation Administration under U.S. Air Force contract FA8721-05-C-0002. Opinions, interpretations, conclusions, and recommendations are those of the authors and are not necessarily endorsed by the U.S. government. The authors appreciate the support and assistance provided by Tony Salmonson (Air Force), John Appleby (Department of Homeland Security), and Neal Suchy (Federal Aviation Administration). The authors gratefully acknowledge the helpful comments received from anonymous reviewers.

References

[1] McLaughlin, M. P., and Zeitlin, A. D., "Safety Study of TCAS II for Logic Version 6.04," MITRE Corp., TR MTR-92W102, McLean, VA, 1992.

[2] McLaughlin, M. P., "Safety Study of the Traffic Alert and Collision Avoidance System (TCAS II)," MITRE Corp., TR MTR-97W32, McLean, VA, June 1997.

[3] Choyce, T. A., and Ciaramella, K. M., "Test and Evaluation of TCAS II Logic Version 7.0," Federal Aviation Administration, Oct. 2000.

[4] *Surveillance, Radar and Collision Avoidance*, ICAO Standards and Recommended Practices, Annex 10, Vol. 4, International Civil Aviation Organization, Montreal, 1998.

[5] Miquel, T., and Rigotti, K., "European Encounter Model," Eurocontrol, TR ACASA/WP1/186/D, Brétigny-sur-Orge, France, March 2002.

[6] Chabert, S., "Safety Encounter Model Focused on Issue SA01A," CENA/Sofréavia and QinetiQ, TR SIRE/WP2/21/D, April 2005.

[7] Hutchinson, H., "Implications on ACAS Performances Due To ASAS Implementation," Eurocontrol, TR IAPA/WP10, Brussels, Belgium, 2005.

[8] Raynaud, B., and Arino, T., "Final Report on the Safety of ACAS II in the European RVSM Environment," Eurocontrol, TR ASARP/WP9/72/D, Brussels, Belgium, 2006.

[9] Kochenderfer, M., Espindle, L., Kuchar, J., and Griffith, J., "Correlated Encounter Model of the National Airspace System," Massachusetts Inst. of Technology Lincoln Lab., Rept. ATC-344, Lexington, MA, Nov. 2008.

[10] "Minimum Operational Performance Standards for Traffic Alert and Collision Avoidance System (TCAS) Airborne Equipment," Radio Technical Commission for Aeronautics, Rept. DO-185A, Washington, D.C., 1997.

[11] Lorenzo, E. J., "Refinement of the TCAS Automated Resolution Advisory Removal Tool," Johns Hopkins Univ. Applied Physics Lab., TR CBH27, Laurel, MD, 2009.

[12] Kochenderfer, M., Kuchar, J., Espindle, L., and Griffith, J., "Uncorrelated Encounter Model of the National Airspace System," Massachusetts Inst. of Technology Lincoln Lab., Rept. ATC-345, Lexington, MA, Nov. 2008.

[13] Edwards, M., Kochenderfer, M., Kuchar, J., and Espindle, L., "Encounter Models for Unconventional Aircraft," Massachusetts Inst. of Technology Lincoln Lab., Rept. ATC-348, Lexington, MA, Jan. 2009.

[14] Billingsley, T. B., Espindle, L. P., and Griffith, J. D., "TCAS Multiple Threat Encounter Analysis," Massachusetts Inst. of Technology, Lincoln Lab., Rept. ATC-359, Lexington, MA, 2009.

[15] Bishop, C. M., *Pattern Recognition and Machine Learning*, Springer–Verlag, New York, 2006.

[16] Neapolitan, R. E., *Learning Bayesian Networks*, Prentice–Hall, Upper Saddle River, NJ, 2004.

[17] Pearl, J., *Probabilistic Reasoning in Intelligent System*, Morgan Kaufmann, San Mateo, CA,1988.

[18] Jensen, F. V., and Nielsen, T. D., *Bayesian Networks and Decision Graphs*, 2nd ed., Springer–Verlag, New York, 2007.

[19] Cormen, T. H., Leiserson, C. E., Rivest, R. L., and Stein, C., *Introduction to Algorithms*, 2nd ed., MIT Press, Cambridge, MA, 2001.

[20] Heckerman, D., "A Tutorial on Learning with Bayesian Networks," Microsoft Research, TR MSR-TR-95-06, Redmond, WA, March 1995.

[21] Heckerman, D., Geiger, D., and Chickering, D. M., "Learning Bayesian Networks: The Combination of Knowledge and Statistical Data," *Machine Learning*, Vol. 20, No. 3, Sept. 1995, pp. 197–243. doi:10.1023/A:1022623210503

[22] Cooper, G. F., and Herskovits, E., "A Bayesian Method for the Induction of Probabilistic Networks from Data," *Machine Learning*, Vol. 9, No. 4, Oct. 1992, pp. 309–347. doi:10.1023/A:1022649401552

[23] Chickering, D. M., "Learning Bayesian Networks is NP-Complete," *Learning from Data: Artificial Intelligence and Statistics V*, edited by D. Fisher and H. Lenz, Springer–Verlag, New York, 1996, pp. 121–130.

[24] Chickering, D. M., "Optimal Structure Identification with Greedy Search," *Journal of Machine Learning Research*, Vol. 3, Nov. 2002, pp. 507–554. doi:10.1162/153244303321897717

[25] Dean, T., and Kanazawa, K., "A Model for Reasoning About Persistence and Causation," *Computational Intelligence*, Vol. 5, No. 2, Aug. 1989, pp. 142–150. doi:10.1111/j.1467-8640.1989.tb00324.x

[26] Murphy, K., "Dynamic Bayesian Networks: Representation, Inference and Learning," Ph.D. Dissertation, Univ. of California, Berkeley, CA, 2002.

[27] "Safety Analysis of Proposed Change to TCAS RA Reversal Logic," Radio Technical Commission for Aeronautics, Rept. DO-298, Washington, D.C., 2005.

[28] Srinivasan, R., *Importance Sampling: Applications in Communications and Detection*, Springer–Verlag, New York, 2002.

[29] Rubinstein, R. Y., *Simulation and the Monte Carlo Method*, Wiley, Hoboken, NJ, 1981.

[30] Kochenderfer, M. J., Espindle, L. P., Kuchar, J. K., and Griffith, J. D., "A Bayesian Approach to Aircraft Encounter Modeling," AIAA Paper 2008-6629, 2008.

[31] May, G., "A Method for Predicting the Number of Near Mid-Air Collisions in a Defined Airspace," *Operational Research Quarterly*, Vol. 22, No. 3, Sept. 1971, pp. 237–251. doi:10.1057/jors.1971.57

[32] Duda, R. O., Hart, P. E., and Stork, D. G., *Pattern Classification*, 2nd ed., Wiley, New York, 2001.

[33] Chludzinski, B., "Lincoln Laboratory Evaluation of TCAS II Logic Version 7," Massachusetts Inst. of Technology Lincoln Lab., Rept. ATC-268, Lexington, MA, 1999.

[34] Chabert, S., and Drévillon, H., "Decision Criteria for Regulatory Measures on TCAS II Version 7.1," Eurocontrol, TR SIRE+/WP7/69/D, Brussels, Belgium, 2008.

[35] Kuchar, J. K., and Drumm, A. C., "The Traffic Alert and Collision Avoidance System," *Lincoln Laboratory Journal*, Vol. 16, No. 2, 2007, pp. 277–296.

[36] Bliss, N. T., Bond, R., Kepner, J., Kim, H., and Reuther, A., "Interactive Grid Computing at Lincoln Laboratory," *Lincoln Laboratory Journal*, Vol. 16, No. 1, 2006, pp. 165–216.

[37] Efron, B., and Tibshirani, R. J., *An Introduction to the Bootstrap*, Chapman & Hall, New York, 1993.

[38] Espindle, L. P., Griffith, J. D., and Kuchar, J. K., "Safety Analysis of Upgrading to TCAS Version 7.1 Using the 2008 U.S. Correlated Encounter Model," Massachusetts Inst. of Technology Lincoln Lab., Rept. ATC-349, Lexington, MA, 2009.

[39] Schaefer, R. J., "A Standards-Based Approach to Sense-and-Avoid Technology," AIAA Paper 2004-6420, Sept. 2004.

[40] Utt, J., McCalmont, J., and Deschenes, M., AIAA Paper 2005-7177, Sept. 2005.

[41] McCalmont, J., Utt, J., Deschenes, M., and Taylor, M., "Sense and Avoid, Phase I (Man-in-the-Loop) Advanced Technology Demonstration," AIAA Paper 2005-7176, Sept. 2005.

[42] Ebdon, M. D., and Regan, J., "Sense-and-Avoid Requirement for Remotely Operated Aircraft (ROA)," Air Combat Command, White Paper OPR: HQ ACC/DR-UAV SMO, Langley AFB, VA, June 2004.

[43] Chen, W.-Z., and Molnar, T. J., "Autonomous Flight Control Sensing Technology (AFCST) Program Phase I—Capability Goals and Sensing Requirements," Air Force Research Lab., TP AFRL-VA-WP-TP-2002-309, Wright–Patterson AFB, OH, July 2002.

[44] Chen, Z.-W., Portilla, E., Clough, B., and Molnar, T. J., "See and Avoid Sensor System Design Part 2—System Reliability & Cost/Benefits", AIAA Paper 2003-6604, Sept. 2003.

[45] Kuchar, J., and Yang, L., "A Review of Conflict Detection and

Resolution Modeling Methods," *IEEE Transactions on Intelligent Transportation Systems*, Vol. 1, No. 4, 2000, pp. 179–189. doi:10.1109/6979.898217

[46] Jones, T., "Tractable Conflict Risk Accumulation in Quadratic Space for Autonomous Vehicles," *Journal of Guidance, Control, and Dynamics*, Vol. 29, No. 1, 2006, pp. 39–48. doi:10.2514/1.10515

[47] Paielli, R. A., and Erzberger, H., "Conflict Probability Estimation for Free Flight," *Journal of Guidance, Control, and Dynamics*, Vol. 20, No. 3, 1997, pp. 588–596. doi:10.2514/2.4081

[48] Yang, L. C., and Kuchar, J. K., "Prototype Conflict Alerting System for Free Flight," *Journal of Guidance, Control, and Dynamics*, Vol. 20, No. 4, 1997, pp. 768–773. doi:10.2514/2.4111

[49] Yang, L., Yang, J. H., Kuchar, J., and Feron, E., "A Real-Time Monte Carlo Implementation for Computing Probability of Conflict," AIAA Paper 2004-4876, 2004.

[50] Arulampalam, M., Maskell, S., Gordon, N., and Clapp, T., "A Tutorial on Particle Filters for Online Nonlinear/Non-Gaussian Bayesian Tracking," *IEEE Transactions on Signal Processing*, Vol. 50, No. 2, Feb. 2002, pp. 174–188. doi:10.1109/78.978374

[51] Shakernia, O., Chen, W.-Z., and Raska, M. V. M., "Passive Ranging for UAV Sense and Avoid Applications," AIAA Paper 2005-7179, Sept. 2005.

[52] Griffith, J. D., Kochenderfer, M. J., and Kuchar, J. K., "Electro-Optical System Analysis for Sense and Avoid," AIAA Paper 2008-7253, 2008.

[53] Kochenderfer, M. J., Griffith, J. D., and Kuchar, J. K., "Electro-Optical Hazard Alerting Using Line-of-Sight Rate," AIAA Paper 2008-6630, 2008.

[54] Temizer, S., Kochenderfer, M. J., Kaelbling, L. P., Lozano-Perez, T., and Kuchar, J. K., "Unmanned Aircraft Collision Avoidance Using Partially Observable Markov Decision Processes," Massachusetts Inst. of Technology Lincoln Lab., Rept. ATC-356, Lexington, MA, 2009.